Bull. Mater. Sci. (2019) 42:107
https://doi.org/10.1007/s12034-019-1814-4

Wollastonite/forsterite composite scaffolds offer better surface for hydroxyapatite formation

R LAKSHMI[1], RAJAN CHOUDHARY[2], DEEPALEKSHMI PONNAMMA[3], KISHOR KUMAR SADASIVUNI[4] and SASIKUMAR SWAMIAPPAN[5,*]

[1]Department of Chemistry, Auxilium College, Vellore, Tamil Nadu 632006, India
[2]Division of Chemistry, Department of Science and Humanities, Saveetha School of Engineering, Saveetha Institute of Medical and Technical Sciences (SIMATS), Chennai, Tamil Nadu 602105, India
[3]Center for Advanced Materials, Qatar University, P.O. Box 2713, Doha, Qatar
[4]Department of Mechanical and Industrial Engineering, Qatar University, P.O. Box 2713, Doha, Qatar
[5]Department of Chemistry, School of Advanced Sciences, Vellore Institute of Technology, Vellore, Tamil Nadu 632014, India
*Author for correspondence (ssasikumar@vit.ac.in)

MS received 16 August 2018; accepted 27 November 2018; published online 4 April 2019

Abstract. The present work deals with a comparative study of ceramic/ceramic composites for the development of scaffolds for biomedical applications. Wollastonite and forsterite were synthesized by a sol–gel combustion method. The influence of constituents and composition on apatite deposition was studied by fabricating wollastonite/forsterite composites. The X-ray diffraction pattern explains the bone like-apatite deposition within early stages of immersion. The atomic force microscopy micrographs revealed that with an increase in wollastonite content in the composites the roughness was enhanced. Dissolution studies further confirmed the rapid consumption of Ca and P ions from the simulated body fluid. Hence, apatite formation was observed to be more on the surface of a composite containing a higher amount of wollastonite. The results suggest that composites have more influence on the biomineralization activity when compared with pure bioceramics.

Keywords. Wollastonite; forsterite; composites; roughness; simulated body fluid; apatite.

1. Introduction

The major requirements for a typical biomaterial are biodegradability, enough strength and excellent efficiency to interact with the surrounding tissues and bones in the body. These criteria can be achieved by developing bioactive porous ceramic–ceramic scaffolds which can trigger the regeneration of new bone tissues and the biomechanical load tolerance during bone formation [1–4]. Forsterite (Mg_2SiO_4) is a bioceramic having mechanical properties superior to hydroxyapatite (HAp) and bioglass [5]. The role of divalent cations like Mg^{2+} in bone remodelling, skeletal development, human metabolism and cellular processes is well established. The *in-vitro* studies of forsterite reveal poor apatite deposition ability and an extremely slow degradation rate [6]. Moreover, the apatite formation on the surface of forsterite can be induced by fabricating its composites [7]. It is reported that nanocrystalline forsterite can enhance the fracture toughness of the bioactive glass matrix without deteriorating its biomineralization properties [8]. The HAp–forsterite–bioactive glass nanocomposite on a 316 litres stainless steel shows an increase in the HAp formation with an increase in the forsterite amount in the composite [9]. Recently, a calcium silicate/HAp nanocomposite has shown improved mechanical properties and bioactivity for HAp with the increase in calcium silicate concentration [10].

There are several reports claiming the enhancement of mechanical properties with the incorporation of forsterite but very few studies have been published to enhance the apatite deposition ability of forsterite bioceramic. Thus, the present work is an attempt to improve the reactivity of forsterite by fabricating its composites with bioactive wollastonite. Wollastonite and forsterite powders were synthesized by the sol–gel combustion method and mixed in different ratios. The properties of composites were compared based on their compositions. The fabricated composites were characterized using different characterization techniques, and the influence of the compositional ratio on the apatite formation ability was evaluated.

2. Materials and method

Sodium chloride (99.9%, AR, SDFCL), sodium bicarbonate, Extrapure (99.5%, AR, SRL), potassium chloride (99.5%, AR, SDFCL), di-potassium hydrogen orthophosphate (99.0%, AR, SDFCL), magnesium chloride (99.0%, AR, SDFCL), hydrochloric acid (35–38%, LR SDFCL), calcium chloride

Table 1. Composition of wollastonite/forsterite composites.

S. no	Code	Composition of wollastonite	Composition of forsterite
1	CC1	80	20
2	CC2	70	30
3	CC3	50	50

(98.0%, AR, SDFCL), sodium sulphate anhydrous (99.5%, AR, SDFCL), Tris(hydroxymethyl)aminomethane (99.8%, AR, SDFCL) and deionized water were used.

2.1 *Preparation of bioceramics*

The detailed procedure followed for the preparation of wollastonite and forsterite is described elsewhere [11,12]. Different ratios of pure wollastonite and forsterite were finely ground using an agate mortar and pestle. The composite was pelletized into a scaffold by a hydraulic pellet press (KBr press). The pressure applied for the preparation of the scaffold was 150 kg cm^{-2}. The dimensions of the scaffold were 13 mm diameter and 2 mm thick. The ratios of wollastonite to forsterite were used to prepare composites and the details are shown in table 1.

2.2 *In vitro biomineralization assessment*

The apatite deposition ability of wollastonite/forsterite scaffolds was studied in simulated body fluid (SBF). The SBF was prepared as per the Kokubo and Takadama protocol. The scaffolds were immersed in 50 ml SBF in a sealed conical flask for 21 days. The samples were incubated without shaking at 37°C and the SBF medium was refreshed after every 24 h. The scaffolds were collected from the solution in different intervals, washed gently with distilled water and dried at 60°C for 1 h using a hot air oven. The formation of HAp on the scaffold surface and variation in surface roughness were characterized by powder X-ray diffraction, Fourier-transform infrared, scanning electron microscopy and atomic force microscopy techniques.

2.3 *Characterization*

The depositions of HAp on the composites were examined by using a powder X-ray diffractometer (Model Bruker, D8 Advance) with Cu Kα radiation. The functional groups in the composites were studied by using a Fourier transform infrared spectrometer (JASCO, 400). The morphology of the composite surface was characterized by using a scanning electron microscope (Carl Zeiss, EVO). The surface roughness before and after HAp deposition studies was analysed using an atomic force microscope (Nanosurf Easyscan 2). The ion concentration of Ca, P, Mg and Si in SBF was examined by inductively coupled plasma optical emission spectroscopy (ICP-OES, Perkin Elmer Optima 5300 DV).

3. Results and discussion

3.1 *Surface analysis of the composites before immersion in SBF*

The FT-IR spectra of the wollastonite/forsterite composites with different ratios (80:20 (CC1); 70:30 (CC2) and 50:50 (CC3)) are shown in figure 1a–c. The absorption band at 475 cm^{-1} corresponds to O–Mg–O bending vibrations. Figure 1c shows that the CC3 sample exhibits a high-intensity peak at 475 cm^{-1} as compared with CC1 and CC2 samples. The peaks in the range of 518 to 620 cm^{-1} and 644 to 685 cm^{-1} are associated with bending vibrations of O–Si–O due to forsterite and wollastonite contents, respectively. The Si–O symmetric stretching was observed at 842 cm^{-1}. The broad band at 902 cm^{-1} was attributed to non-bridging Si–O–Ca. The symmetric stretching vibrations of Si–O–Si were found at 1012 cm^{-1}. These functional groups correspond to the presence of both wollastonite and forsterite in the composites [11,12]. The CC1 composite shows an irregular morphology with micro-pores, cracks and flake-like crystals on the surface (figure 1d). The CC2 composite (figure 1e) exhibits an irregular morphology while the CC3 composite (figure 1f) shows an uneven morphology.

3.2 *Surface roughness analysis*

The surface topography of the composite was examined by AFM. Figure 2 represents the 2D topographical view of wollastonite/forsterite composites. The surface of the CC1 composite (figure 2a) appears to have tiny circular particles distributed over the surface while the CC2 composite (figure 2c) shows bunches of particles distributed over the surface. In the case of CC3, the particles were found to possess different dimensions due to aggregation (figure 2e). The surface roughness of composites was found to be 206.94 (CC1), 180.89 (CC2) and 108.6 nm (CC3). Among all three composites, CC1 shows the maximum surface roughness.

3.3 *XRD analysis*

The XRD patterns (figure 3) of the wollastonite/forsterite composites after immersion in SBF indicate the formation of apatite on their surface. The surface of the CC1 composite was covered by HAp within 7 days of immersion. The apatite peaks exactly match with the JCPDS card no. 01-074-0566 associated with the HAp phase. The peaks appeared more prominently at $2\theta = 32.31$, 26.22, 40.03, 49.89 and 53.50° respectively corresponding to the (2 1 1), (0 0 2), (3 1 0), (2 1 3) and (0 0 4) planes of HAp. The wollastonite and forsterite peaks were not observed on the surface of the scaffold which confirms the complete coverage of the HAp layer

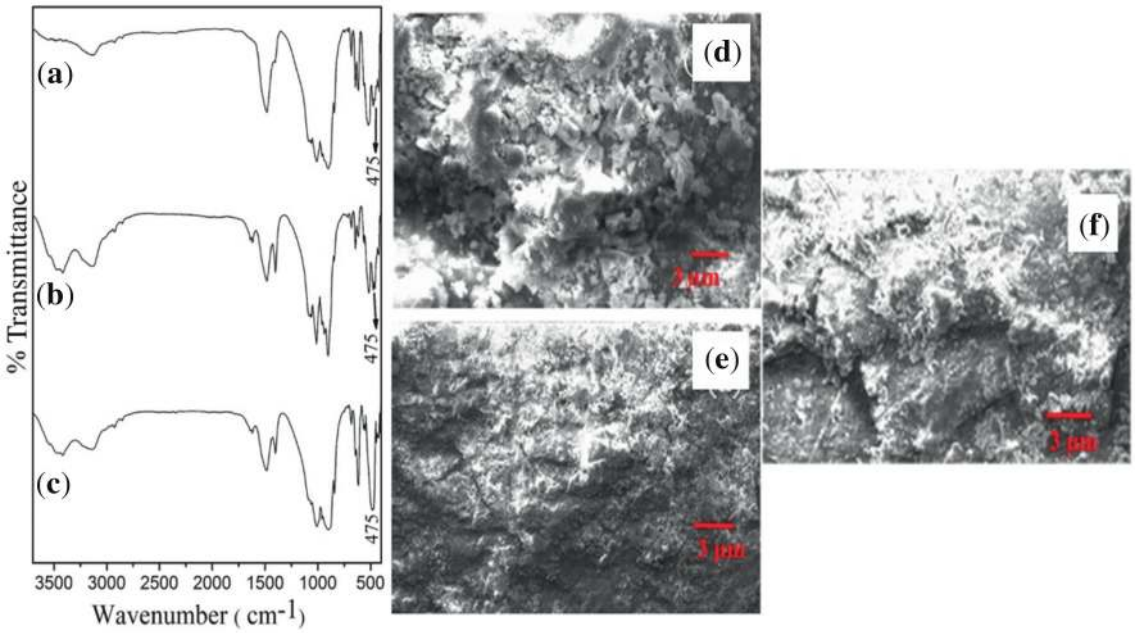

Figure 1. FT-IR spectra and SEM micrographs of (**a**, **d**) CC1, (**b**, **e**) CC2 and (**c**, **f**) CC3 composites.

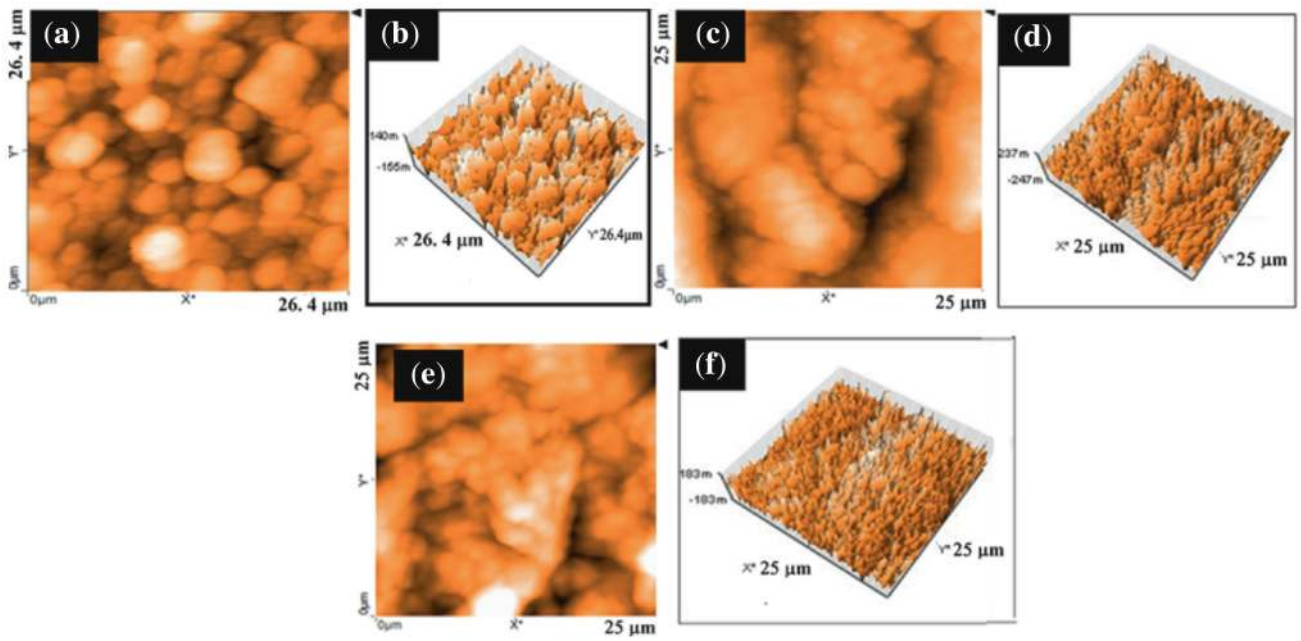

Figure 2. AFM images of composites (**a**, **b**) CC1, (**c**, **d**) CC2 and (**e**, **f**) CC3 before biomineralization studies.

on the surface of the CC1 composite. An increase in the intensity of the HAp peak was noticed as the immersion time was extended from 14 to 21 days.

A similar observation was detected in the XRD pattern of the CC2 composite showing the presence of apatite peaks within 7 days of immersion. It was also noticed that the surface of the CC2 composite comprises dual phases associated with forsterite and apatite. Hence, when the CC2 composite was further immersed in SBF for 21 days, a sharp increase in the intensity of HAp peaks was observed. This indicates that the consumption of necessary ions from the SBF facilitated the deposition of the Ca–P layer covering the entire surface of the CC2 composite.

The CC3 composite shows slow apatite formation when compared with CC1 and CC2. After one week of immersion, the surface of the CC3 composite was composed of apatite

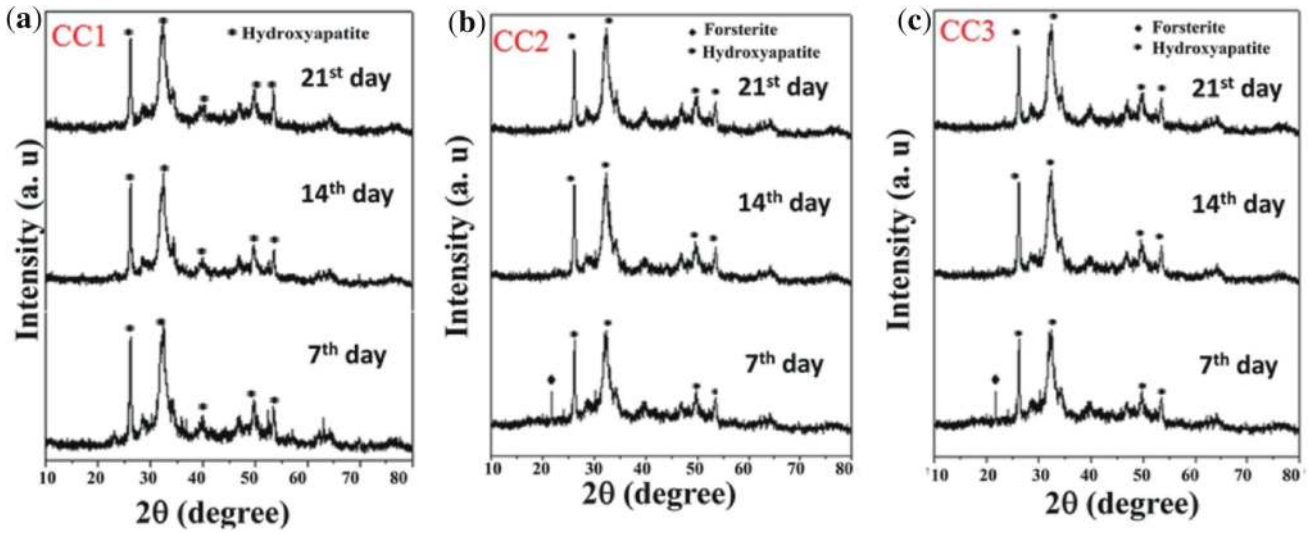

Figure 3. XRD pattern of composites (CC1, CC2 and CC3) after immersion in SBF.

phase accompanied by wollastonite and forsterite (figure 3). The influence of the immersion time (14 days) on apatite deposition indicates that the surface of the CC3 composite was completely covered by the amorphous apatite layer. The deposited HAp matches with the standard JCPDS card no. 01-072-1243. It was also observed that with the increase in the immersion time (21 days) the intensity of HAp peaks enhanced. The literature suggests that forsterite has very less apatite formation ability while wollastonite has remarkable apatite formation ability over other silicate bioceramics [13]. Thus, the current work shows that the apatite deposition ability of forsterite can be improved by preparing its composites with wollastonite.

The variation in biomineralization activity on the surface of composites can be related to the change in their compositional ratio. From the above observation, it can be concluded that an increase in the wollastonite content enhanced the apatite deposition ability of the composites and viceversa. Therefore, the combination of bioactive wollastonite with the superior surface properties of forsterite resulted in remarkable bone-like apatite precipitation on the surface of composites.

3.4 *SEM/EDX analysis of the composites after immersion in SBF*

The surface morphology and elemental composition of wollastonite/forsterite composites after immersion in SBF were analysed. The surface of the CC1 composite was covered by small HAp particles. The deposited HAp was found to be highly homogeneous having a spheroidal-like morphology (figure 4a). The CC2 composite reveals the clusters of HAp particles on the surface (figure 4c). The agglomerated spherical morphology was observed in the case of the CC3 composite (figure 4e). The variations in the surface morphology of composites were due to the difference in their apatite

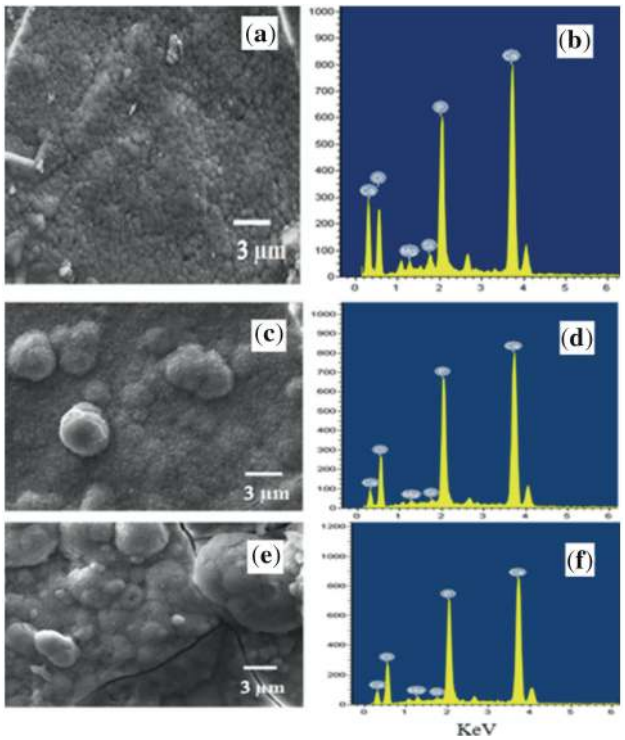

Figure 4. SEM and EDX patterns of (**a**, **b**) CC1, (**c**, **d**) CC2 and (**e**, **f**) CC3 composites after immersion in SBF.

deposition rate. The appearance of the phosphate peak in the EDX spectra of composites further confirms the apatite precipitation (figure 4b, d and f).

3.5 *AFM analysis*

The surface of composites has shown a significant difference in their topography after HAp deposition (figure 5). The

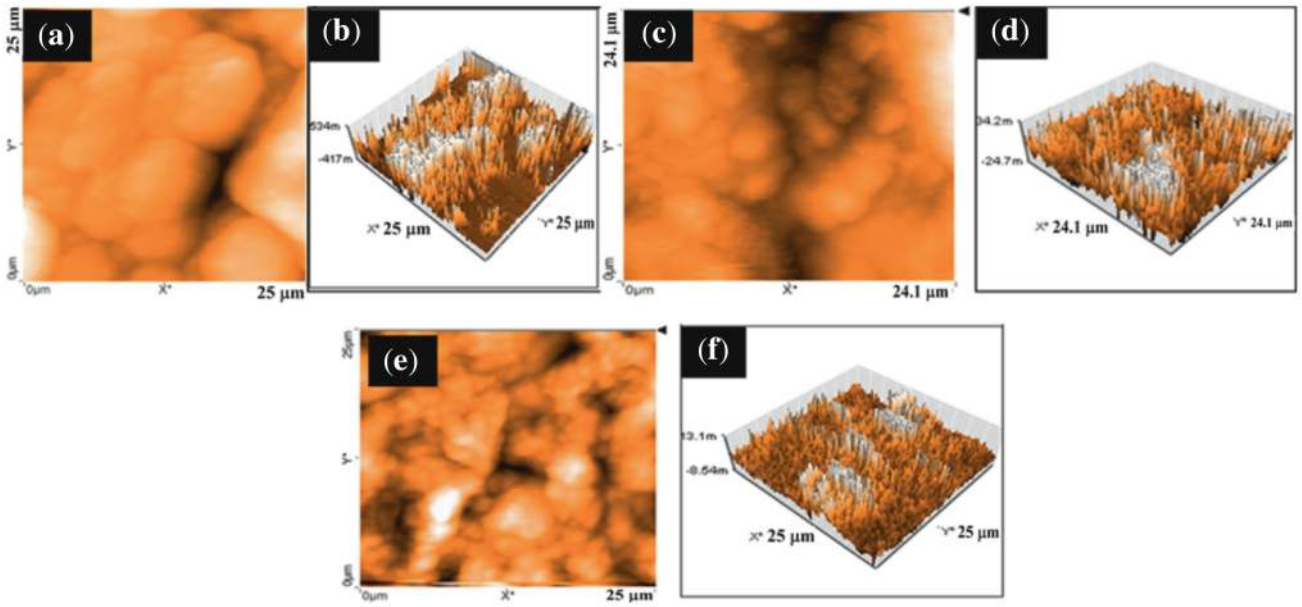

Figure 5. AFM images of (**a**, **b**) CC1, (**c**, **d**) CC2 and (**e**, **f**) CC3 composites after immersion in SBF.

Table 2. Surface roughness value of wollastonite/forsterite composites.

S. no	Wollastonite/forsterite composite	Before HAp deposition, nm	After HAp deposition, nm
1	CC1	206.9	2126.6
2	CC2	180.8	1906.5
3	CC3	108.6	1874.2

increase in the size of the particles observed on the surface of the CC1 composite was due to a faster growth of apatite particles (figure 5a). This led to the increase in the surface roughness of the composite. A similar pattern was noticed for CC2 and CC3 composites as well. The surface roughness values of composites after apatite deposition are tabulated in table 2. The major reason for such variations in their surface roughness values was due to the rate at which apatite deposition took place. The faster the apatite deposition, the higher the roughness noticed. These results indicate that the deposition rate also affects the surface properties of the materials.

3.6 *Dissolution analysis*

The variations in the activity of wollastonite/forsterite composites were further studied by their dissolution behaviour in SBF. It has been suggested that the dissolution analysis plays a major role in predicting the biological response of materials in the physiological environment [14,15]. ICP-OES analysis was carried out to examine the concentration of Ca, Si, P and Mg ions released/consumed during apatite deposition by the wollastonite/forsterite composites. The ion release kinetics of the CC1 composite (figure 6a) shows a drastic change in Ca and P ions from 103 to 74 ppm and 42 to 23 ppm while an increase in the concentration of Mg ions was found (from 30 to 47 ppm). The calcium and phosphorus ions are considered as necessary ions responsible for apatite deposition. Hence, the continuous consumption of calcium and phosphorus ions decreased their concentration in the SBF. Magnesium is not required for apatite formation, as a result, an increase in its concentration was detected throughout the immersion period. In addition, Si ions were negligibly leached out from the composites.

A uniform reduction in the concentration of Ca and P ions was observed till the end of biomineralization studies (figure 6b). The calcium concentration decreased from 99 to 75 ppm while 40 to 20 ppm was detected in the case of phosphorus. This dissolution response was found comparably similar to the CC1 composite and confirms the precipitation of HAp on the surface of the CC2 composite. The release profile of the magnesium ion in the SBF was found to increase constantly (27–45 ppm) showing its negligible utilization in apatite deposition. Moreover, no significant change in the Si level was observed in the SBF.

Figure 6c shows a distinct dissolution profile of the CC3 composite in the SBF. The poor consumption of calcium and phosphorus ions from the medium resulted in slow apatite formation activity of the CC3 composite. The reason for the sudden change in the activity was due to the higher compositional ratio of forsterite in the CC3 composite when compared with other composites and thus the SBF was enriched in magnesium ions. Previous findings state that magnesium retards the apatite deposition ability of a bioceramic.

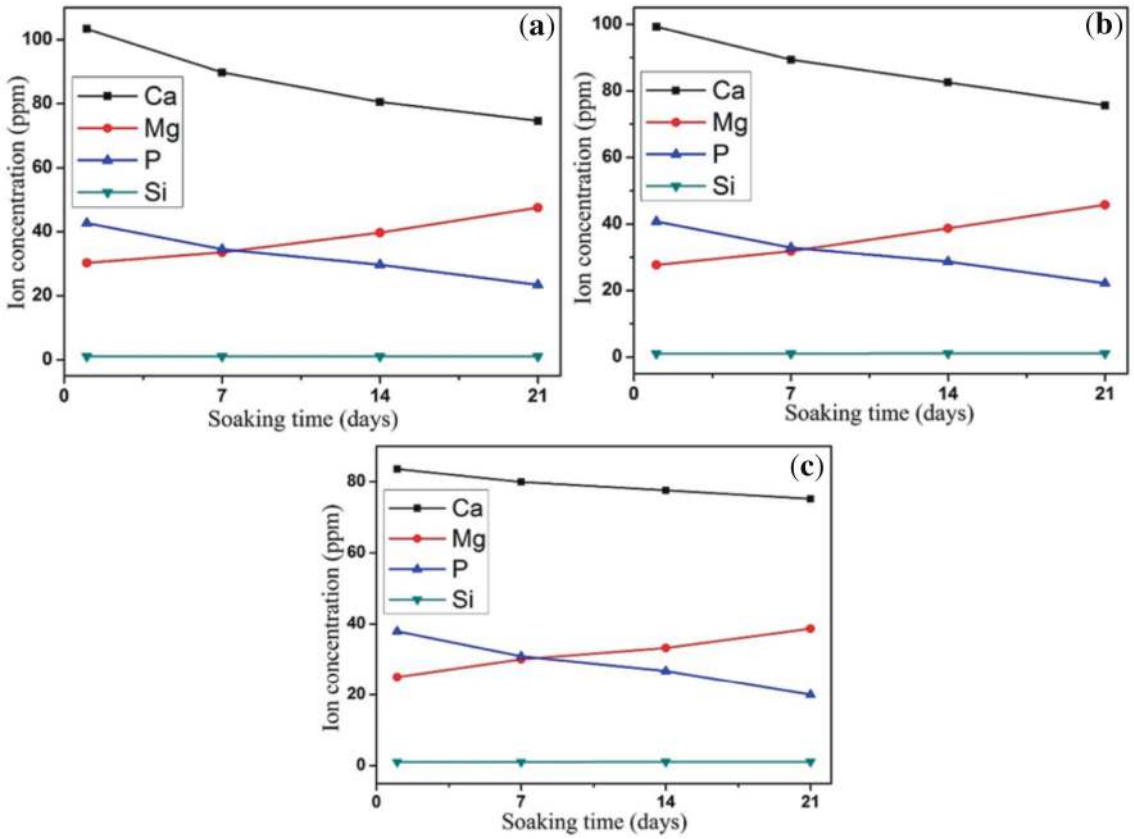

Figure 6. Ionic concentration of (**a**) CC1, (**b**) CC2 and (**c**) CC3 composites during immersion in SBF.

The magnesium ion delays the crystallization rate of the amorphous Ca–P film and suppresses the conversion of amorphous $CaO-P_2O_5$ into stable apatite [16]. The literature states that the β-wollastonite/forsterite composites containing 50 and 70% calcium silicate were more suitable candidates for bone repairing application [7]. But current work suggests that 80% wollastonite content can also be a desirable composite. In order to confirm this notion, a detailed cellular investigation of these composites is required. These results show that chemical composition also plays a vital role in determining the apatite deposition ability of bioceramics.

The dissolution analysis confirmed that the CC1 composite exhibited good HAp deposition ability compared to other composites. This was found in concordance with the XRD analysis of the composite surface after immersion (figure 3). As the compositional ratio of forsterite in composites was increased the apatite deposition ability affected. The presence of wollastonite in composites was found to exert more influence on *in-vitro* biomineralization. Hence, the incorporation of forsterite nanopowders in the bioactive wollastonite matrix has influenced the apatite formation ability of the wollastonite/forsterite composite.

The wollastonite/forsterite composites undergo several interfacial reactions during immersion in SBF. The detailed mechanism of these reactions is explained as follows. When the composites are immersed in SBF, an ion exchange step is initiated. This process causes the exchange of alkali earth ions (Ca^{2+} and Mg^{2+}) from the composites with hydrogen ions present in the SBF. This leads to the breakdown of the silica network into silanol at the interface of the composites. The silanol further undergoes a polycondensation reaction with hydroxyl ions (OH^-) from the SBF to form a silica-rich layer ($Si-O^-$) with the elimination of water. Studies reveal that the silica-rich layer provides necessary sites to induce apatite nucleation [17]. Therefore, an increase in silica linkages on the surface might provide the possibility of forming more amounts of the silica-rich layer. The silica groups present in the composites are found to be more when compared with wollastonite ($CaO{\cdot}SiO_2$) or forsterite ($2MgO{\cdot}SiO_2$) alone. The negatively charged silica-rich layer attracts cations (Ca^{2+}) from the SBF and later anions (PO_4^{2-}) to initiate Ca–P formation at the interface. The concentration of calcium and phosphorus ions in the SBF can be correlated with the dissolution studies showing a constant decrease after 7 days (figure 6). This process continues, leading to deposit an amorphous $CaO-P_2O_5$ film. Later, carbonate and hydroxyl anions crystallize the film into calcium deficient hydroxycarbonate apatite [18]. This indicates that the silicon content also plays a vital role in apatite deposition on the surface of silicate bioceramics [19]. Therefore, the chemical constituents,

compositional ratio and dissolution rate were found to play a vital role in examining the biomineralization ability of wollastonite/forsterite composites.

4. Conclusion

In this study, different ratios of wollastonite/forsterite bioceramic composites were fabricated. *In-vitro* biomineralization studies reveal the formation of the HAp layer on the surface of wollastonite/forsterite composites. It was also found that the CC1 composite shows higher HAp deposition ability when compared to CC2 and CC3 composites, as it contains more amounts of wollastonite. SEM studies disclose the irregular morphology of wollastonite/forsterite composites before *in-vitro* studies. After apatite deposition, the agglomerated spherical morphology was observed for the composite. We demonstrated that the composites containing 80% wollastonite content increase the surface roughness and enhance the apatite formation ability of forsterite.

Acknowledgements

The authors thank DST-FIST for the XRD, SEM facility and SAIF/IIT Madras for ICP-OES facility. This study was financially supported by Vellore Institute of Technology Research Grants for Engineering, Management and Science (VITRGEMS).

References

[1] Deng J, Li P, Gao C, Feng P, Shuai C and Peng S 2014 *Mater. Manuf. Process.* **29** 877
[2] Sopyan I, Gunawan Shah Q H and Mel M 2016 *Manuf. Process.* **31** 713
[3] Ilyuschenko A, Okovity V A, Shevtsov A I, Kashin N G and Kulak A I 2002 *Mater. Manuf. Process.* **17** 177
[4] Sopyan I, Nawawi N A, Shah Q H, Ramesh S, Tan C Y and Hamdi M 2011 *Mater. Manuf. Process.* **26** 908
[5] Kharaziha M and Fathi M H 2009 *Ceram. Int.* **35** 2449
[6] Ni S and Chang J 2009 *J. Biomater. Appl.* **24** 139
[7] Ni S, Chou L and Chang J 2008 *J. Mater. Sci. Mater. Med.* **19** 359
[8] Dinarvand P, Seyedjafari E, Shafiee A, Jandaghi A B, Doostmohammadi A, Fathi M H *et al* 2011 *ACS Appl. Mater. Interfaces* **3** 4518
[9] Sebdani M M and Fathi M H 2012 *Ceram. Int.* **38** 1325
[10] Beheri H H, Mohamed K R and El-Bassyouni G T 2013 *Mater. Des.* **44** 461
[11] Lakshmi R and Sasikumar S 2012 *Adv. Mater. Res.* **584** 479
[12] Choudhary R, Manohar P, Vecstaudza J, Yáñez-Gascón M J, Pérez Sánchez H, Nachimuthu R *et al* 2017 *Mater. Sci. Eng. C* **77** 811
[13] Lin K L, Zhai W Y, Chang J, Zeng Y and Qian W J 2005 *Ceram. Int.* **31** 323
[14] García-Páez I H, Pena P, Baudin C, Rodríguez M A, Cordoba E and De Aza A H 2016 *Bol. Soc. Esp. Ceram. V.* **55** 1
[15] Choudhary R, Vecstaudza J, Krishnamurithy G, Balaji Raghavendran H R, Murali M R, Kamarul T *et al* 2016 *Mater. Sci. Eng. C* **68** 89
[16] Vallet-Regi M, Salinas A J, Roman J and Gil M 1999 *J. Mater. Chem.* **9** 515
[17] Liu X, Ding C and Chu P K 2004 *Biomaterials* **25** 1755
[18] Kim H M, Himeno T, Kokubo T and Nakamura T 2005 *Biomaterials* **26** 4366
[19] Hou X, Yin G, Chen X, Liao X, Yao Y and Huang Z 2011 *Appl. Surf. Sci.* **257** 3417